

Low-intensity UV effects on optical constants of PMMA film

M. Rashidian · D. Dorrnian

Received: 13 December 2013 / Accepted: 20 February 2014 / Published online: 23 April 2014
© The Author(s) 2014. This article is published with open access at Springerlink.com

Abstract Effects of low-intensity UV treatment on the optical constants of red BS dye-doped polymethyl methacrylate (PMMA) film including refractive index, extinction coefficient, real and imaginary parts of dielectric constant, band gap energy, Urbach energy, and refractive index dispersion parameters are measured and calculated. Changes in optical constants mainly occurred in the UV–VIS range. Red BS dye, which is used as a UV absorber impurity in PMMA films, generated another energy band gap which was increased by UV treatment. Although some of the optical constants of PMMA are not changed noticeably by the treatment in this low range of UV radiation, our results confirm that polymeric changes such as chain scission and depolymerization can directly affect the optical constants of PMMA.

Keywords PMMA · UV · Optical constants · Band gap energy · Urbach energy · Wemple–Didomenico model · Cauchy–Sellmeier model

Introduction

Poly(methyl methacrylate) (PMMA) is one of the best organic optical materials widely used to make a variety of optical devices, such as optical lenses. It is known that its refractive index changes upon UV irradiation, which provides a means to fabricate structures, such as gratings or waveguides. Thus, the optical characteristic of PMMA

is at the focal point of consideration. However, polymers are widely influenced by UV radiation. Radiations, especially in this range of short wave lengths, can change the polymer optical characteristics. Up to now, many studies on photo-induced refractive index change under irradiation from UV lamps concentrated on PMMA containing either photochemically active dopants or residual monomer have been reported [1]. Further investigation in this direction is warranted as it may provide a practical solution to realize low-cost fabrication of polymeric devices [2–6].

UV radiation initiates photophysical and photochemical processes in polymers, but its influence is restricted to a thin surface layer, because our experiments are done on PMMA thin films. Here, we have used red BS dye as an impurity in PMMA films as a powerful UV absorber. Organic compounds contained in polymer films, even in trace amounts, affect the reactions occurring during irradiation. They can act as sensitizers or initiators of polymer photodegradation, or sometimes stabilize the system. Interesting contributions concern the impact of UV irradiation on the properties of PMMA thin films obtained by a spin-coating technique [2, 7].

In this work, the effect of UV radiation on the optical properties of red BS dye-doped PMMA film is studied experimentally. Optical spectra are analyzed to determine optical constants such as refractive index, extinction coefficient, dielectric constant and optical conductivity. Optical constants such as refractive index, absorption coefficient and dielectric constant can be analyzed by transmittance and reflectance spectra.

Optical band gap, Urbach energy and the nature of transition are also determined using optical absorption spectra. We investigate the optical properties of these complexes, so that this information would help

M. Rashidian (✉) · D. Dorrnian
Science and Research Branch, Laser Laboratory,
Plasma Physics Research Center, Islamic Azad University,
Tehran, Iran
e-mail: m.rashidan@gmail.com

researchers toward applying these materials in optical communication and optical devices. The study of optical absorption, particularly absorption edge, has proved to be very useful for elucidation of the optical properties and optical constants of these materials. It is possible to determine the indirect and direct transition occurring in the band gap of the sample by optical absorption spectra. The dissipation factor and optical conductivity are also calculated.

The manuscript is organized as follows: following the “Introduction” in the first section, the “Experimental setup” is described in the second section. The third section is devoted to the “Results and discussion” and the “Conclusion” is presented in the final section.

Experimental setup

The red BS dye-doped PMMA film was prepared by dissolving PMMA powder in dichloromethane solvent. PMMA powder was provided by Yazd Polymer Talaei (YPT) Co., Tehran, Iran. 20 g PMMA powder with 1 g red BS dye was dissolved in 200 ml dichloromethane. The viscous solvent was poured on a plane glass in a closed box. The solution was dried in a closed atmosphere at room temperature for 24 h to obtain 0.2 mm thickness red BS dye-doped PMMA film. One part of the dye-doped PMMA film was exposed to a low-pressure mercury lamp TUV 30 W (G30T8 Philips) at room temperature in a closed atmosphere of an aluminum box for 2 days. There was a 10 cm distance between the lamp and samples and the lamp emitted radiation of 253.7 nm wavelength at 21 mW/cm². The change in the absorbance spectrum of the samples was measured by a Varian Cary-500 spectrophotometer at room temperature.

Results and discussion

Refractive index

The spectral distribution of transmittance T and reflectance R were measured using unpolarized light at normal incidence in the wavelength range of 200–2,000 nm. The transmittance spectra of thin films are shown in Fig. 1. The reflectance of samples is approximately constant <0.1 in the whole range.

The optical parameters of the samples can be started to characterize from the complex refractive index:

$$n = n(\omega) + ik(\omega) \quad (1)$$

where n is its real part and k is its imaginary part. n can be obtained from [8]

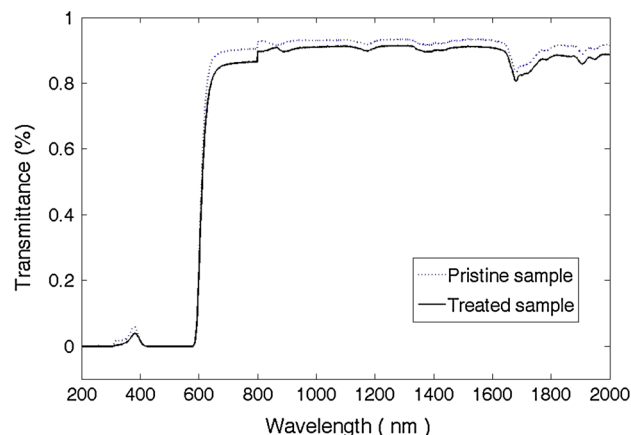


Fig. 1 Transmittance spectrum of samples

$$n = \left(\frac{1+R}{1-R} \right) + \sqrt{\frac{4R}{(1-R)^2} - k^2}, \quad (2)$$

in which $k = \lambda\alpha/4\pi$. Transmission and reflection of the samples can be converted to the absorption coefficient using

$$\alpha = \frac{1}{d} \ln \left[\frac{(1-R)^2}{2T} + \sqrt{\frac{(1-R)^4}{4T^2} + R^2} \right] \quad (3)$$

where α is the absorption coefficient and d is the thickness of the sample. The values of n for UV-treated and pristine samples are shown in Fig. 2. In the visible range of electromagnetic spectrum, the refractive index n of both samples is below 1.45. This value of the refractive index of samples is much lower than that of hard amorphous hydrogenated carbon samples, which is in the visible range from 1.9 to 2.3. The magnitude of refractive index for UV-treated sample is increased in the UV and visible range, while this magnitude is decreased in the IR range. In Fig. 3, the imaginary part of the refractive index k for

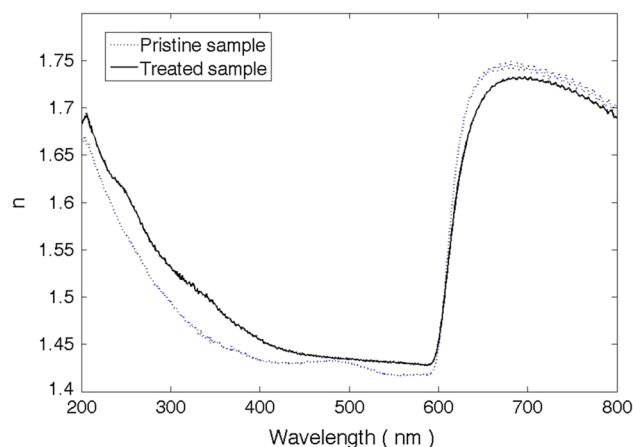


Fig. 2 The real part of refractive index



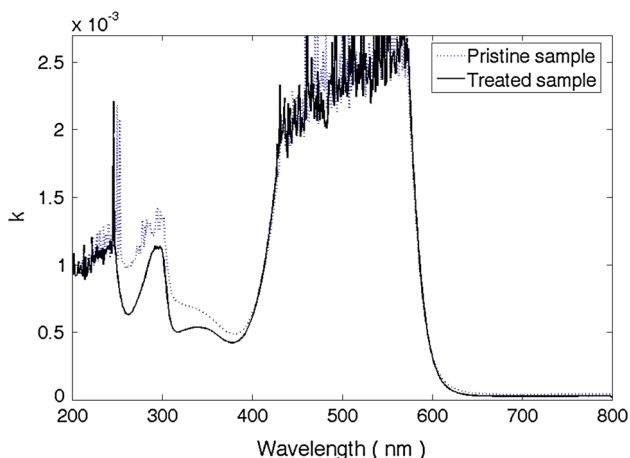


Fig. 3 The imaginary part of refractive index of samples

UV-treated and pristine samples is shown. As can be seen, k is decreased in the UV range (in 250–400 nm wavelength) in the case of UV-treated sample and remains unchanged in the other ranges.

The Wemple and DiDomenico model can be used to explain the behavior of refractive index in the range of wavelengths, where the light absorption is relatively low [9]. In this model by using a single oscillator description, the frequency-dependent dielectric constant is used to define the dispersion energy parameters E_0 and E_d . Dispersion plays an important role in the research of optical materials, because it is a significant factor in optical communication and designing devices for spectral dispersion. It is observed that for pristine PMMA sheet, there is anomalous dispersion at $\lambda > 800$ nm as well as normal dispersion at $\lambda < 800$ nm. In the anomalous dispersion region, there are many peaks indicating the anomalous behavior of refractive index. This behavior obeys the multioscillator model rules. In the normal dispersion region, the refractive index dispersion was analyzed using the single model developed by Wemple and DiDomenico. In addition, for the treated sample, there is no anomalous dispersion when $\lambda < 800$. The variation of n and k values in the investigated frequency range shows that some interactions take place between photons and electrons. The refractive index dispersion for crystallized and amorphous materials can be expressed as [10]:

$$n^2 = 1 + \frac{E_d E_0}{E_0^2 - (hv)^2} \tag{4}$$

where n is the real part of refractive index, hv is the photon energy, E_0 is the average excitation energy for electronic transitions and E_d is the dispersion energy, which is a measure of the strength of interband optical transitions. This model describes the dielectric response for transitions below the optical gap.

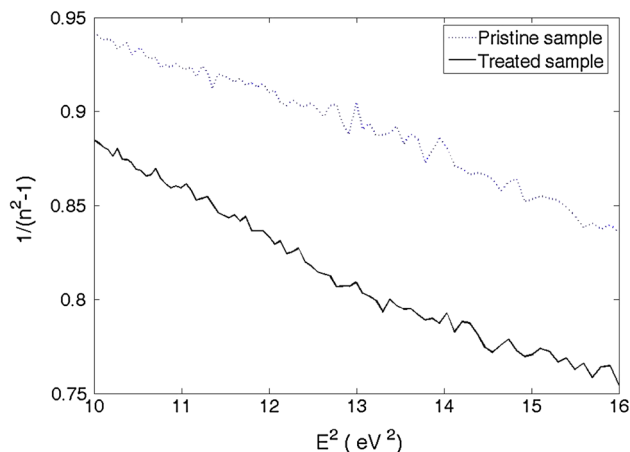


Fig. 4 Plot of $1/(n^2 - 1)$ versus (hv)

Table 1 Optical parameters of samples

Film	E_0 (eV)	E_d (eV)	M_{-1} (eV)	M_{-3} (eV) ⁻²	n_∞	λ_0 (nm)	S_0 (m ⁻²)
Pristine	7.26	7.73	1.16	0.021	1.38	150.9	4.06×10^{13}
Treated	7.43	8.68	1.06	0.020	1.40	142.2	5.02×10^{13}

The plot of $1/(n^2 - 1)$ vs. $(hv)^2$ allows us to determine the oscillator parameters. E_0 and E_d values are determined from the slope and intercept on the vertical axis of Fig. 4. The refractive index for $hv < E_0$ states a smoothly decreasing function with increasing λ without peaks, as shown in Fig. 2. This decrease in the refractive index can be associated with fundamental band gap absorption.

The dielectric constant of the material can be calculated using the dispersion relation of incident photon. The refractive index is also fitted using a function for extrapolation toward shorter wavelengths. These data corresponding to the wavelength range lying below the absorption edge of the material are used. Therefore, the refractive index can also be analyzed to determine the long wavelength refractive index (n_∞), average oscillator wavelength (λ_0) and oscillator length strength S_0 of the thin film. To determine these values, we use the single term Sellmaier oscillator [11] in which n varies as:

$$\frac{n_\infty^2 - 1}{n^2 - 1} = 1 - \left(\frac{\lambda_0}{\lambda}\right)^2 \tag{5}$$

n_∞ and λ_0 values are obtained from the linear parts of $1/(n^2 - 1)$ vs. λ^{-2} and are given in Table 1. Rearranging Eq. 5 gives [12]:

$$n^2 - 1 = \frac{S_0 \lambda_0^2}{1 - \lambda_0^2/\lambda^2} \tag{6}$$

where $S_0 = (n_\infty^2 - 1)/\lambda_0$. The S_0 value for the thin film is calculated.

The single oscillator parameters E_0 and E_d can be related to the imaginary part of complex dielectric constant, and M_{-1} and M_{-3} , moments of the optical spectra for the samples are expressed as [13]:

$$E_0^2 = \frac{M_{-1}}{M_{-3}} \quad \text{and} \quad E_d^2 = \frac{M_{-1}^3}{M_{-3}} \quad (7)$$

The M_{-1} and M_{-3} moments are calculated using Eq. 7 and are presented in Table 1. The oscillator energy E_0 is independent of the scale of ϵ_2 , the imaginary part of dielectric constant, and is consequently an average energy gap, in contrast to E_d which depends on ϵ_2 . The results of our experiments for pristine and UV-treated red BS dyedoped PMMA show that the magnitude of both single oscillator parameters increased by UV treatment; in other words, we have a stronger contribution of lattice vibrations to the refractive index due to UV treatment.

Changes in the magnitude of $n_\infty^2 = \epsilon_\infty$, λ_0 and S_0 after UV treatment are presented in Table 1. The long wavelength refractive index n_∞ of treated film as well as the average oscillator strength S_0 increased after the treatment. These changes show that the PMMA films are suitable for changing the refractive index efficiently by photo-irradiation. Changing these two parameters has a potential applicability for optical devices like channel waveguides and photo-optical switching devices.

For photon energies less than the energy gap ($h\nu < E_g$), the refractive index dispersion curves are fitted by Cauchy–Sellmeier model [14]:

$$n = n_0 + n_1 E^2 \quad (8)$$

where n_0 and n_1 are constants and E is the photon energy. The plots of n vs. E^2 are shown in Fig. 5. n_0 and n_1 values are calculated from the slope and intercept of the plots and are given in Table 2. In fact, n_1 is the nonlinear refractive index which shows the effect of E^2 in samples. This quantity is increased by UV treatment.

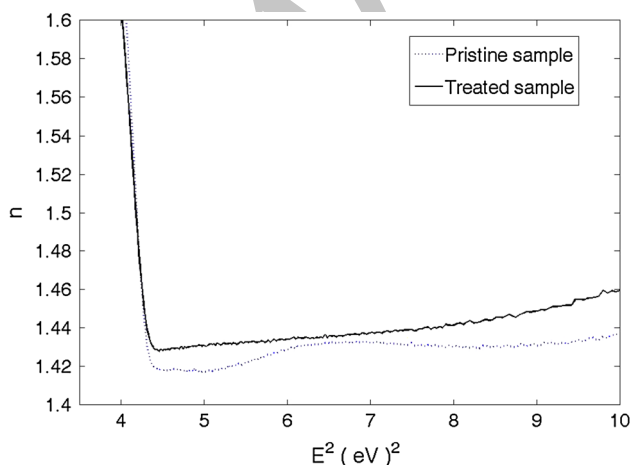


Fig. 5 Plot of n versus E^2 for pristine and UV-treated samples

Table 2 Optical parameters of samples

Film	E_{1g} (eV)	E_{2g} (eV)	E_{u1} (eV)	E_{u2} (eV)	n_0	n_1
Pristine	2.017	3.625	1.82	0.044	1.3333	0.0092
Treated	2.017	3.714	2.38	0.046	1.3553	0.0112

Determination of optical band gap

In the range of wavelengths where a sharp increase of absorption appears in the substance, the Tauc relation for dependence of absorbance on wavelength or photon energy applies. The optical band gap is the value of optical energy gap between the valance band and the conduction band. The optical band gap of the samples is determined from the absorption spectra near the absorption edges. The photon absorption in many amorphous materials is found to obey the Tauc relation [15, 16], which is of the form:

$$\alpha h\nu = B(h\nu - E_g)^m \quad (9)$$

where α is the absorption coefficient, $h\nu$ is the photon energy and B is a factor that depends on the transition probability and can be assumed to be constant within the optical frequency range. The index m is related to the distribution of the density of states. The index m has discrete values like $1/2$, $3/2$, 2 or more depending on whether the transition is direct or indirect and allowed or forbidden, respectively. In the direct and allowed cases, the index $m = 1/2$, whereas for the direct but forbidden cases it is $3/2$. But for the indirect and allowed cases $m = 2$ and for the forbidden cases it is three or more [17]. The value of m for our samples is estimated from the slope of the $\log(\alpha)$ vs. $\log(h\nu)$ plots by taking a linear fit and is found to be 2. To calculate E_g , the usual method is plotting $(\alpha h\nu)^{1/m}$ against $h\nu$, which is presented in Fig. 6. The values of the band gap energy of pristine and treated samples are found to be 2.017 eV, where it remained unchanged under UV radiation, while the optical gap due to absorption of red BS dye increased from 3.625 to 3.714 eV, confirming that red BS dye is a good UV absorber.

Studying the optical absorption spectra of the films shows that the absorption spectra mechanism is due to indirect transition. The optical band gap E_{1g} of the PMMA film is not changed in the treatment process due to low power of the applied UV radiation, but E_{2g} which belongs to the red BS dye particles in PMMA varies in the UV radiation process. In fact, E_{2g} decreases noticeably in the UV-treated sample.

Urbach spectral tail in the films

The absorption tail of the films was investigated in the studied energy range. The spectral dependence of the

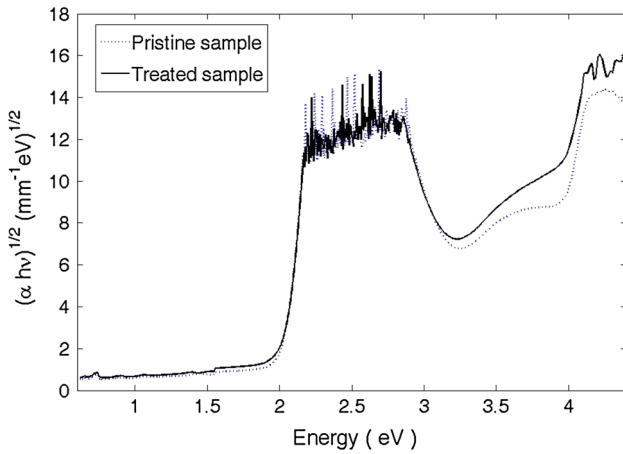


Fig. 6 The $(\alpha hv)^{1/2}$ versus photon energy (hv)

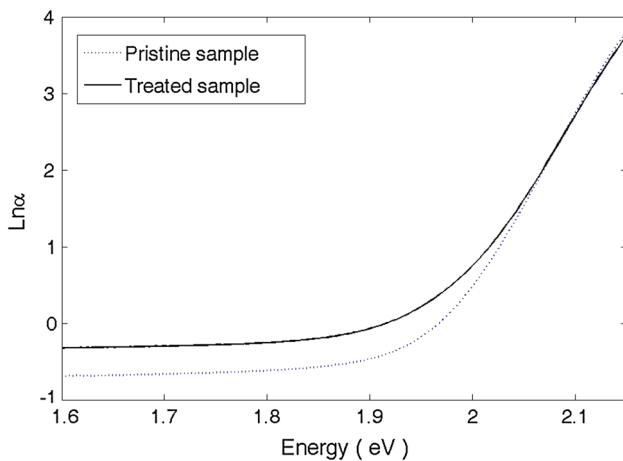


Fig. 7 The $\ln(\alpha)$ versus photon energy (hv)

absorption coefficient α was studied at photon energies less than the energy gap of the films, i.e., in the region of the so-called Urbach spectral tail, where the absorption coefficient α falls off exponentially with decreasing photon energy E , and it is expressed as:

$$\alpha = \alpha_0 \exp(E/E_u) \tag{10}$$

Each of the absorption edges from Fig. 7 exhibits two different exponential regions with different slopes. It is found that the spectral dependence of the logarithm of absorption coefficient for each region shown is combined from two linear functions [18]:

$$\alpha = \alpha_{01} \exp(E/E_{u1}) + \alpha_{02} \exp(E/E_{u2}) \tag{11}$$

where α_{01} and α_{02} are parameters which are dependent on photon energy. E_{u1} for region I and E_{u2} for region II in Urbach plots are Urbach energies, as shown in Fig. 7. In the low-energy region the spectral dependence of logarithm of absorption coefficient is characterized by a small slope (E_{u1} energy), followed by an extremely large slope (E_{u2}

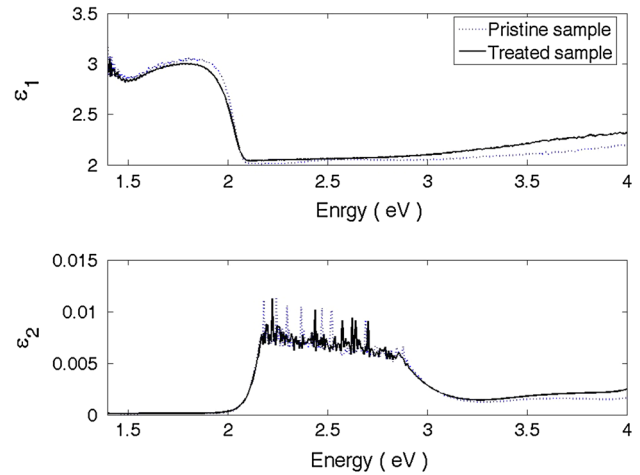


Fig. 8 The real part ϵ_1 and imaginary part ϵ_2 of dielectric constant of samples versus photon energy for pristine and UV-treated samples

energy). The Urbach energies (E_{u1} and E_{u2}) are introduced in Table 2.

It is seen that the Urbach energies E_{1u} and E_{2u} increase in treated films, indicating an increase in disorder in PMMA films.

Dielectric properties

One of the most important basic dielectric parameters, which plays a major role in the determination of material properties is the permittivity or dielectric constant. This in turn is related to the dipole moment, polarizability, molecular radius, specific and molar refraction, relaxation time, wave impedance, specific and molar dispersivity, dielectric susceptibility, etc. The permittivity as described before is calculated using Maxwell's equation for electromagnetic radiation ($\epsilon = n^2$).

The complex dielectric constant is described as $\epsilon^* = \epsilon_1 + i\epsilon_2$ where ϵ_1 is the real part and ϵ_2 is the imaginary part of the dielectric constant. The imaginary and real parts of dielectric constant are expressed as [19]:

$$\epsilon_1 = n^2 - k^2 \tag{12}$$

and

$$\epsilon_2 = 2nk \tag{13}$$

The real part of the dielectric constant relates to the dispersion, while the imaginary part provides a measure of the dissipative rate of the wave in the medium. The dielectric properties of the films change with refractive index.

Figure 8a, b shows the real and imaginary parts' dependence on wavelength, respectively.

As can be seen in the case of UV-treated samples, the real part of dielectric constant is increased in the range of

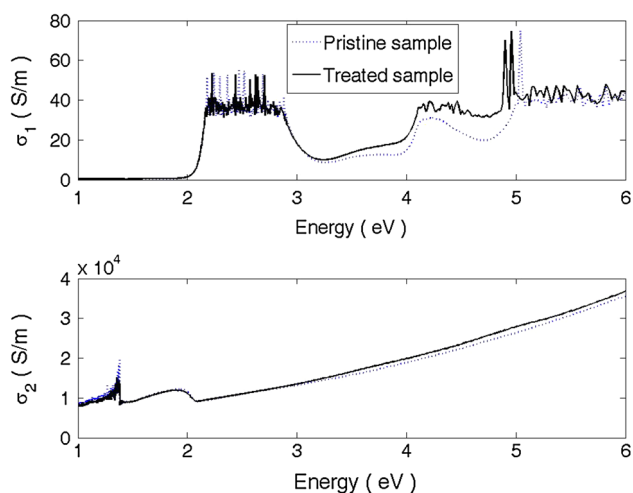


Fig. 9 The real part σ_1 and imaginary part σ_2 of optical conductivity constant versus photon energy for pristine and UV-treated samples

UV–VIS of electromagnetic spectrum, but this parameter is decreased in the NIR range. It suggests that dielectric loss increases after treatment. The imaginary part of dielectric constant is increased in the 250–400 nm range.

Optical conductivity of the films

The complex optical conductivity ($\sigma^* = \sigma_1 + i\sigma_2$) is related to the complex dielectric constant ($\epsilon^* = \epsilon_1 + i\epsilon_2$) by [19]:

$$\sigma_1 = \omega\epsilon_2\epsilon_0 \cdot \sigma_2 = \omega\epsilon_1\epsilon_0 \quad (14)$$

where ω is the angular frequency and ϵ_0 is the free space dielectric constant. The real σ_1 and imaginary σ_2 parts of the optical conductivity as a function of photon energy are plotted in Fig. 9a and b. One can see that the optical conductivity increases with increasing energy. Increase in optical conductivity is due to electrons excited by photon energy. The optical conductivity of the complexes changes due to the formation coordination of the complex. The optical conductivity does not indicate any certain trend with atomic number ion in the complexes.

In addition, the absorption coefficient can be used to calculate the optical conductivity as follows:

$$\sigma = \frac{\alpha nc}{4\pi} \quad (15)$$

where α is the absorption coefficient and c is the velocity of light in vacuum.

Conclusion

In this research, the effect of non-polarized low-intensity UV beam on the optical parameters of PMMA thin film is

investigated. This is the starting point of a project on studying the effect of high-intensity pulsed UV laser treatment on these parameters. The refractive index of samples n are computed from the obtained reflection and transmission spectrum. On the basis of the optical investigations of the films, the following results are obtained. Other optical constants such as extinction coefficient k and dielectric constant ϵ are calculated for the films.

It is found that the refractive index values of films are decreased with wavelength in the visible range. The change of n is a criterion of structure change and our results confirm that in this low power of radiation the UV-treated sample can undergo photochemical structural changes.

All these changes, some of which are too small but some are not negligible, are due to the well-known effects of UV radiation on PMMA. UV irradiation leads to PMMA degradation. Chain scission and depolymerization occur in PMMA film, and according to our other analysis other reactions such as destruction of side groups and oxidation can also be seen in the UV-treated film. In the intermolecular interactions, UV radiation breaks the carbon–chlorine bonds. The chlorine radicals formed during photolysis of these compounds are capable of abstracting hydrogen atoms from PMMA chains, and further secondary reactions subsequently occur. Although we cannot yet say which of these polymeric mechanisms directly affect the optical characteristics of PMMA, we believe that this is a promising field which will have a wide range of applications in the optic industry.

Open Access This article is distributed under the terms of the Creative Commons Attribution License which permits any use, distribution, and reproduction in any medium, provided the original author(s) and the source are credited.

References

1. Yu, J., Tao, X., Tamb, H.Y., Demokan, M.S.: Modulation of refractive index and thickness of poly(methyl methacrylate) thin films with UV irradiation and heat treatment. *Appl. Surf. Sci.* **252**, 1283 (2005)
2. Migah, M.D., Zidan, H.M.: Influence of UV-irradiation on the structure and optical properties of polycarbonate films. *Curr. Appl. Phys.* **6**, 91 (2006)
3. Cabuk, S., Simsek, S.: First-principles studies of the electronic structure and optical properties of AgBO₃ (B = Nb, Ta) in the paraelectric phase. *Cent. Eur. J. Phys.* **6**, 730 (2008)
4. Kirillova, M.M., Magnitskaya, M.V., Makhnev, A.A., Lobov, I.D., Nomerovannaya, L.V., Tsvyashchenko, A.V., Fomicheva, L.N.: The electronic structure and optical and magneto-optical properties of the CaCo₂ compound synthesized at a high pressure: experiment and theory. *J. Exp. Theor. Phys.* **100**, 983 (2005)
5. Srivastava, S., Haridas, M., Basu, J.K.: Optical properties of polymer nanocomposites. *Bull. Mater. Sci.* **31**, 213 (2008)
6. Andrade-Filho, T., Ribeiro, T.C.S., Del Nero, J.: The UV–vis absorption spectrum of the flavonol quercetin in methanolic solution: a theoretical investigation. *Eur. Phys. J. E* **29**, 253 (2009)

7. Kaczmarek, H., Chaberska, H.: The influence of solvent residue, support type and UV-irradiation on surface morphology of poly(methyl methacrylate) films studied by atomic force microscopy. *Polym Test.* **27**, 736 (2008)
8. Dragoman, D., Dragoman, M.: *Optical characterization of solids*, 1st edn. Springer, Berlin (2002)
9. Wemple, S.H., DiDomenico, M.: Behavior of the electronic dielectric constant in covalent and ionic materials. *Phys. Rev. B* **3**, 1338 (1971)
10. DiDomenico, M., Wemple, S.H.: Oxygen-octahedra ferroelectrics. I. theory of electro-optical and nonlinear optical effects. *J. Appl. Phys.* **40**, 720 (1969)
11. Wolaton, A.K., Moss, T.S.: Determination of refractive index and correction to effective electron mass in PbTe and PbSe. *Proc. Roy. Soc.* **81**, 509 (1963)
12. Lee, P.A., Said, G., Davis, R., Lim, T.H.: On the optical properties of some layer compounds. *J. Phys. Chem. Solids* **30**, 2719 (1969)
13. Wemple, S.H., DiDomenico, M.: Optical dispersion and the structure of solids. *Phys. Rev. Lett.* **23**, 1156 (1969)
14. Subrahmanyam, N.A.: *Textbook of optics*, 9th edn. Brij Laboratory, Delhi (1977)
15. Yakuphanoglu, F., Barim, G., Erol, I.: The effect of FeCl₃ on the optical constants and optical band gap of MBZMA-co-MMA polymer thin films. *Physica B* **391**, 136 (2007)
16. Saravanan, S., Anantharaman, M.R., Venkatachalam, S., Avasthi, D.K.: Studies on the optical band gap and cluster size of the polyaniline thin films irradiated with swift heavy Si ions. *Vacuum* **82**, 56 (2007)
17. Yakuphanoglu, F., Arslan, M.: Determination of thermo-optic coefficient, refractive index, optical dispersion and group velocity parameters of an organic thin film. *Physica B* **393**, 304 (2007)
18. Yakuphanoglu, F., Cukurovali, A., Yilmaz, I.: Refractive index and optical absorption properties of the complexes of a cyclobutane containing thiazolyl hydrazone ligand. *Opt. Mater.* **27**, 1363 (2005)
19. Wiktorezyk, T.: Preparation and optical properties of holmium oxide thin films. *Thin Solid Films* **405**, 238 (2002)

Archive of SID